



MIT Open Access Articles

Computational ghost imaging

The MIT Faculty has made this article openly available. **Please share** how this access benefits you. Your story matters.

Citation	Shapiro, Jeffrey H. "Computational ghost imaging." Lasers and Electro-Optics, 2009 and 2009 Conference on Quantum Electronics and Laser Science Conference. CLEO/QELS 2009. Conference on. 2009. 1-2. © 2010 IEEE.
As Published	http://ieeexplore.ieee.org/stamp/stamp.jsp?tp=&arnumber=5225024
Publisher	Institute of Electrical and Electronics Engineers
Version	Final published version
Citable link	http://hdl.handle.net/1721.1/61419
Terms of Use	Article is made available in accordance with the publisher's policy and may be subject to US copyright law. Please refer to the publisher's site for terms of use.

Computational Ghost Imaging

Jeffrey H. Shapiro

Research Laboratory of Electronics, Massachusetts Institute of Technology, Cambridge, MA 02139, USA
jhs@mit.edu

Abstract: A computational ghost-imaging arrangement that uses only a single-pixel detector is described. It affords a new 3D sectioning capability and matches the resolution of pseudothermal ghost imaging.

© 2009 Optical Society of America

OCIS codes: (110.4980) Partial coherence in imaging; (270.5290) Photon statistics; (030.1640) Coherence.

Ghost imaging is the acquisition of object information by means of photocurrent correlation measurements. It has been demonstrated with biphoton light [1] and pseudothermal light [2]. Recently [3], we established a Gaussian-state analysis of ghost imaging that unified prior work on biphoton and pseudothermal sources. Our analysis indicated that ghost-image formation is intrinsically due to classical coherence propagation. Other recent work [4], however, has ascribed pseudothermal-light ghost imaging to nonlocal two-photon quantum interference. We will show [5] that ghost imaging can be accomplished with only *one* detector, viz., the bucket detector that collects a single pixel of light which has interacted with the object. As only one light beam and one photodetector are required, this imaging configuration cannot depend on nonlocal two-photon interference. Moreover, it affords a new 3D sectioning capability.

Consider the pseudothermal-light lensless ghost imaging setup shown in the left panel of Fig. 1, in which $E_S(\boldsymbol{\rho}, t)e^{-i\omega_0 t}$ and $E_R(\boldsymbol{\rho}, t)e^{-i\omega_0 t}$ are scalar, positive frequency, classical signal and reference fields with $\sqrt{\text{photon/s}}$ units and center frequency ω_0 . They are the outputs from 50-50 beam splitting of $E(\boldsymbol{\rho}, t)e^{-j\omega_0 t}$, a continuous-wave (cw) laser beam that has been transmitted through a rotating ground-glass diffuser. The signal and reference undergo paraxial diffraction over L -m-long free-space paths, yielding measurement-plane fields with baseband envelopes $E_1(\boldsymbol{\rho}, t)$ and $E_2(\boldsymbol{\rho}, t)$. The field $E_1(\boldsymbol{\rho}, t)$ illuminates a shot-noise limited pinhole photodetector centered at $\boldsymbol{\rho}_1$ with sensitive region $\boldsymbol{\rho} \in \mathcal{A}_1$. The field $E_2(\boldsymbol{\rho}, t)$ illuminates an amplitude-transmission mask $T(\boldsymbol{\rho})$, located immediately in front of a shot-noise limited bucket photodetector with sensitive region $\boldsymbol{\rho} \in \mathcal{A}_2$. The photocurrents from these detectors are AC-coupled into a correlator that time averages their product to estimate their ensemble-average cross correlation, $C(\boldsymbol{\rho}_1)$, as the pinhole detector is scanned over the plane. Pseudothermal light is well modeled as a narrowband classical Gaussian random process with a coherence-separable, Gaussian-Schell model correlation structure. It follows that the ghost image cross-correlation function in the far field of that spatially incoherent source is given by [3]:

$$C(\boldsymbol{\rho}_1) = q^2 \eta^2 A_1 \left(\frac{2P}{\pi a_L^2} \right)^2 \int_{\mathcal{A}_2} d\boldsymbol{\rho} e^{-|\boldsymbol{\rho}_1 - \boldsymbol{\rho}|^2 / \rho_L^2} |T(\boldsymbol{\rho})|^2, \quad (1)$$

for a transparency that lies within the a_L -radius illuminated region. In this expression: q is the electron charge; η is the photodetector quantum efficiency; A_1 is the pinhole area; P is the photon flux of the source; and $a_L = \lambda_0 L / \pi \rho_0$ and $\rho_L = \lambda_0 L / \pi a_0$ give the image-plane intensity radius and coherence radius, respectively, in terms of their source-plane counterparts, a_0 and $\rho_0 \ll a_0$, and the laser wavelength λ_0 . Equation (1) shows that the pseudothermal ghost image is erect, with spatial resolution set by ρ_L .

It is now possible to identify two new configurations for lensless ghost imaging. The first is shown in the right panel of Fig. 1. We transmit a cw laser beam through an idealized spatial light modulator (SLM) consisting of $d \times d$ pixels arranged in a $(2M + 1) \times (2M + 1)$ array with 100% fill factor within a $D \times D$ opaque pupil, where $D = (2M + 1)d$ and $M \gg 1$. This SLM imposes a phase $\phi_{nm}(t)$ on the light transmitted through pixel (n, m) , with $\{e^{i\phi_{nm}(t)} : -M \leq n, m \leq M\}$ being independent identically-distributed random processes obeying $\langle e^{i\phi_{nm}(t)} \rangle = 0$ and $\langle e^{i[\phi_{nm}(t_2) - \phi_{jk}(t_1)]} \rangle = \delta_{jn} \delta_{km} e^{-|t_2 - t_1| / T_0}$, where the coherence time T_0 is long compared to the response times of the AC-coupled photodetectors. In this source's far field, $E_1(\boldsymbol{\rho}, t)$ and $E_2(\boldsymbol{\rho}, t)$ will have intensity widths $\sim \lambda_0 L / d$ and coherence lengths $\sim \lambda_0 L / D$. Furthermore, Central Limit Theorem considerations imply that $E_1(\boldsymbol{\rho}, t)$ and $E_2(\boldsymbol{\rho}, t)$ may be taken to be jointly Gaussian. Hence our SLM configuration will produce a ghost image of spatial resolution $\lambda_0 L / D$ within a spatial region of width $\lambda_0 L / d$. This ghost imager could use noise generators to drive the SLM, but it is more interesting to employ strong sinusoidal modulation, $\phi_{nm}(t) = \Phi \cos[(\Omega_0 + \Delta\Omega_{nm})t]$, with different $\Delta\Omega_{nm}$ for each pixel.

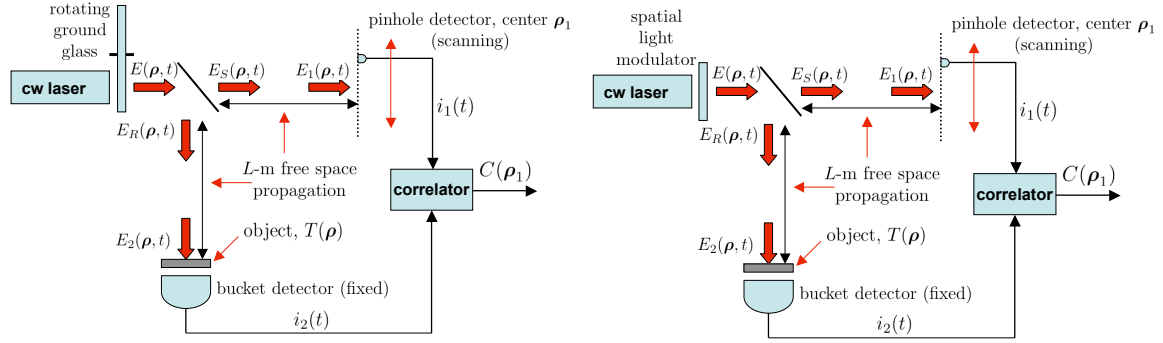


Fig. 1. Left panel: configuration for pseudothermal lensless ghost imaging. Right panel: configuration for spatial light modulator lensless ghost imaging

The configuration for computational ghost imaging, shown in Fig. 2, uses deterministic modulation of a cw laser beam to create the field $E_2(\rho, t)$ that illuminates the object transparency, after which it is collected by a bucket (single-pixel) detector. Knowing the deterministic modulation allows us to use diffraction theory to *compute* the intensity pattern that would have illuminated the pinhole detector in the usual lensless ghost imaging configuration. The time-average correlation function, between the AC-coupled photodetector output and the mean-value subtracted computed intensity pattern, $\Delta\tilde{I}_1(\rho_1, t)$, will then be a background-free ghost image with spatial resolution $\lambda_0 L/D$ over a spatial extent of width $\lambda_0 L/d$. Because only one photodetector has been employed, this computational ghost image cannot be due to nonlocal two-photon interference.

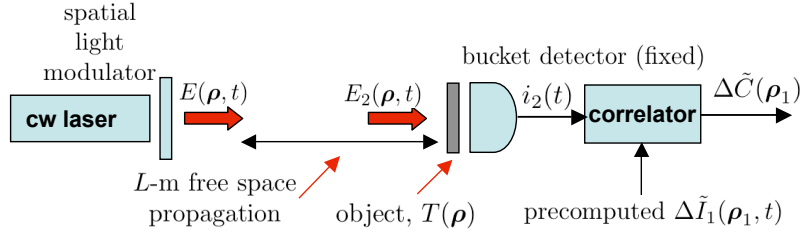


Fig. 2. Configuration for computational lensless ghost imaging.

Computational ghost imaging obviates the need for a high spatial-resolution detector. In addition, it permits 3D sectioning to be performed. To see that this is so, consider the depth of focus for the pseudothermal case, i.e., how badly its ghost image is blurred if the object is at $z = L$ but the pinhole detector is at $z = L + \Delta L$. In the near-field of the pre-diffuser laser beam, it turns out that this focal region is a very small fraction of the source-to-object path [5]. Consequently, the pseudothermal ghost imager can only image one focal region at a time for a range-spread object viewed in reflectance. However, because the computational ghost imager can precompute $\Delta\tilde{I}_1(\rho_1, t)$ for a wide range of propagation distances, the same bucket-detector photocurrent can be correlated with many such $\Delta\tilde{I}_1(\rho_1, t)$ to perform 3D sectioning of the object's reflectance.

In conclusion, we have introduced two new ghost imaging configurations: spatial light modulator and computational ghost imaging. The latter only needs a single-pixel detector and enables 3D sectioning to be performed.

This work was supported by the U. S. Army Research Office, the DARPA Quantum Sensors Program, and the W. M. Keck Foundation for Extreme Quantum Information Theory.

References

1. T. B. Pittman, Y. H. Shih, D. V. Strekalov, and A. V. Sergienko, Phys. Rev. A **52**, R3429 (1995).
2. A. Valencia, G. Scarcelli, M. D'Angelo, and Y. Shih, Phys. Rev. Lett. **94**, 063601 (2005); F. Ferri, D. Magatti, A. Gatti, M. Bache, E. Brambilla, and L. A. Lugiato, Phys. Rev. Lett. **94**, 183602 (2005).
3. B. I. Erkmen and J. H. Shapiro, Phys. Rev. A **77**, 043809 (2008).
4. R. Meyers, K. S. Deacon, and Y. Shih, Phys. Rev. A **77**, 041801(R) (2008); Y. Shih, arXiv:0805.1166 [quant-ph].
5. J. H. Shapiro, arXiv:0807.2614 [quant-ph].